Case Studies in Structural Engineering 7 (2017) 1–23

Contents lists available at ScienceDirect

Case Studies in Structural Engineering

journal homepage: www.elsevier.com/locate/csse

Case Study

Seismic vulnerability assessment of an Italian historical masonry dry dock

Marco Zucca*, Pietro Giuseppe Crespi, Nicola Longarini

Dept. of Architecture, Built Environment and Construction Engineering, Politecnico di Milano, Italy

ARTICLE INFO

Article history:
Received 10 November 2015
Received in revised form 1 November 2016
Accepted 3 November 2016
Available online 6 November 2016

Keywords:
Dry dock
Seismic vulnerability
Earthquake
Finite element analysis

ABSTRACT

The paper presents the seismic vulnerability analysis of the military dry dock built in 1861 inside the Messina's harbor. The study appears very important not only for the relevance of the dry dock itself, but also for its social, military and symbolic role. As a first step, the historical documentation about the dry dock delivered by the Military Technical Office, in charge of its maintenance, was thoroughly examined. This activity was fundamental to understand the construction methods, the rehabilitation works executed after the severe earthquake of 1908 and, finally, the works carried out to increase the size of the dry dock in 1950. After this first step, numerical seismic analyses were done with some implemented finite element models (FEM) of the structure. In each FEM, the vertical loads were applied according to the "construction stages" analysis technique, in order to achieve an appropriate representation of the soil stresses around the structure. The analysis results were evaluated according to the Italian design code (NTC 2008) in order to determine the seismic vulnerability of the dry dock.

© 2016 The Authors. Published by Elsevier Ltd. This is an open access article under the CC BY-NC-ND license (http://creativecommons.org/licenses/by-nc-nd/4.0/).

1. Introduction

The dry dock studied in this paper is a part of the Navy dockyard in Messina (Sicily island, Italy). The arsenal is composed of a few complex buildings and plants devoted to construction, maintenance and repairing works of Navy vessels, including all the owned weapons and equipment. The arsenal includes all sorts of workshops, experimental laboratories, warehouses and administrative-management offices. The former idea to build an arsenal in Messina can be attributed to the Arab dominion in Sicily.

Since the sixteenth century, historians, writers, chroniclers and scholars of Messina have always taken for granted that Messina had a large arsenal, really defined "*the most important in the Mediterranean*". That was justified by many resources of city's history: the city had a strong seafaring and commercial vocation and it was in the center of the main maritime trade for a couple of millennia being a compulsory transit point on the busiest routes.

The dry dock located inside the Messina's arsenal is a gravity type one; it is called "*Masonry basin*" and nowadays it is used by the "*Agenzia Industrie Difesa Militare*". According to the chronicles, it was built with many difficulties. A campaign of surveys carried out in 2003 revealed a stratigraphic sequence of unusual heterogeneous materials in the quoin of the internal dock maybe in order to counter water and slime infiltration emerged during the excavation.

* Corresponding author.
E-mail addresses: marco.zucca@polimi.it (M. Zucca), pietro.crespi@polimi.it (P.G. Crespi), nicola.longarini@polimi.it (N. Longarini).

http://dx.doi.org/10.1016/j.csse.2016.11.001
2214-3998/© 2016 The Authors. Published by Elsevier Ltd. This is an open access article under the CC BY-NC-ND license (http://creativecommons.org/licenses/by-nc-nd/4.0/).

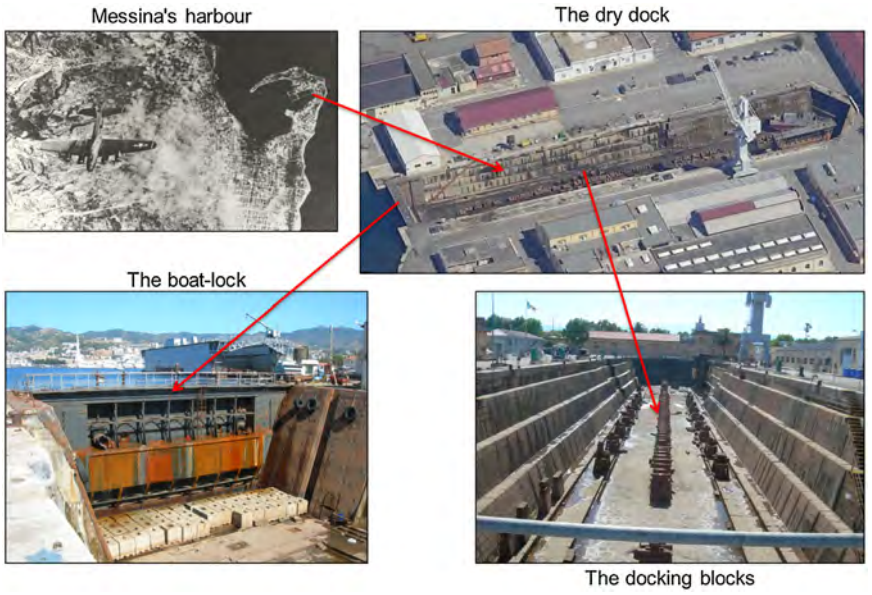

Fig. 1. Dry Dock.

The stone cladding (thickness of about 80 cm) rests on a pozzolanic conglomerate (about 70 cm), cast as a water infiltration barrier on the base slab. Two rows of bricks were used as a sub-base for finished paving. The pozzolanic mixture used (lime, crushed stone and pozzolan) was "poor" of pozzolan and "rich" in lime, therefore it was used as a binder of gravel and like general inert material. The obtained conglomerate allows water filtration, compromising the serviceability of the basin. The thickness of the foundation mat is about 4.00 m.

This structure was severely damaged under the strong famous earthquake that struck Messina in 1908, with the natural consequence of inactivity of the basin up to 1911.

The new structure was built about 1.70 m out-off-axis with respect to the former one. Its slab was investigated in the 2005 by a test campaign highlighting the thickness (about 5 m) and the good quality of the materials. This slab rests on a layer of stones, varying between 0.90 and 1.80 m, shaped as an upward concave surface. The walls of the out-off-axis new section are covered by blocks, packed with the natural conglomerate (polygenic conglomerate in slang pudding) founded and removed during the excavation executed by using mines.

Along the longitudinal axis of the new basin there are not drainage tunnels, even present in the section of the "old dock", but there are drains and pipes laid under the extrados of the slab.

In 1976, the "*Genio Civile*" realized the last important reinforcement of the basin. The so-called "gargame" area located at the entrance of the dry dock was covered by steel plates (thickness of 15 mm) with tie beams on both the North and South fronts, close to the entrance threshold (Fig. 1).

2. Brief historical notes

The first buildings and activities in the Messina's harbor date from the roman period and had a strong development during the Arabian domination in Sicily (827–1019 A.D.). From the urbanistic point of view, the complex of the structures is located in an area detached from the city and it is provided by suitable defensive works to protect the military activities.

As military shipyard, the dry dock was built few years after the Italian Unification (1861). In those years, there was an increase in size and tonnage of ships; the increase was supported by the use of advanced steel technologies in both ships and steam engines construction. Therefore, the development of a dry dock was possible because it was requested to set up a suitable area well equipped for the maintenance of military and merchant ships.

The structural works began in 1869 and after seven years the dry dock construction was completed. The dry dock, planned as a large basin with 104 m length, 36.50 m width and 9.90 m height walls (with a total height of 15.90 m including the 6.00 m thickness of the foundation mat), covering an area of 21500 m^2. The works continued without interruption until 1908 when the well-known earthquake of Messina damaged the structure of the dock's lock device: the dry dock was flooded and a ship that was there in maintenance sank. After the restoration works, the dry dock was reopened in 1912. After the Second World War, the dry-dock needed to be enlarged owing to the increase of the international economy, resulting in an intensification of the ships traffic and by the use of larger size ships. In 1954, the enlargement works of the dry dock ended and its final length grew of about 50 m.

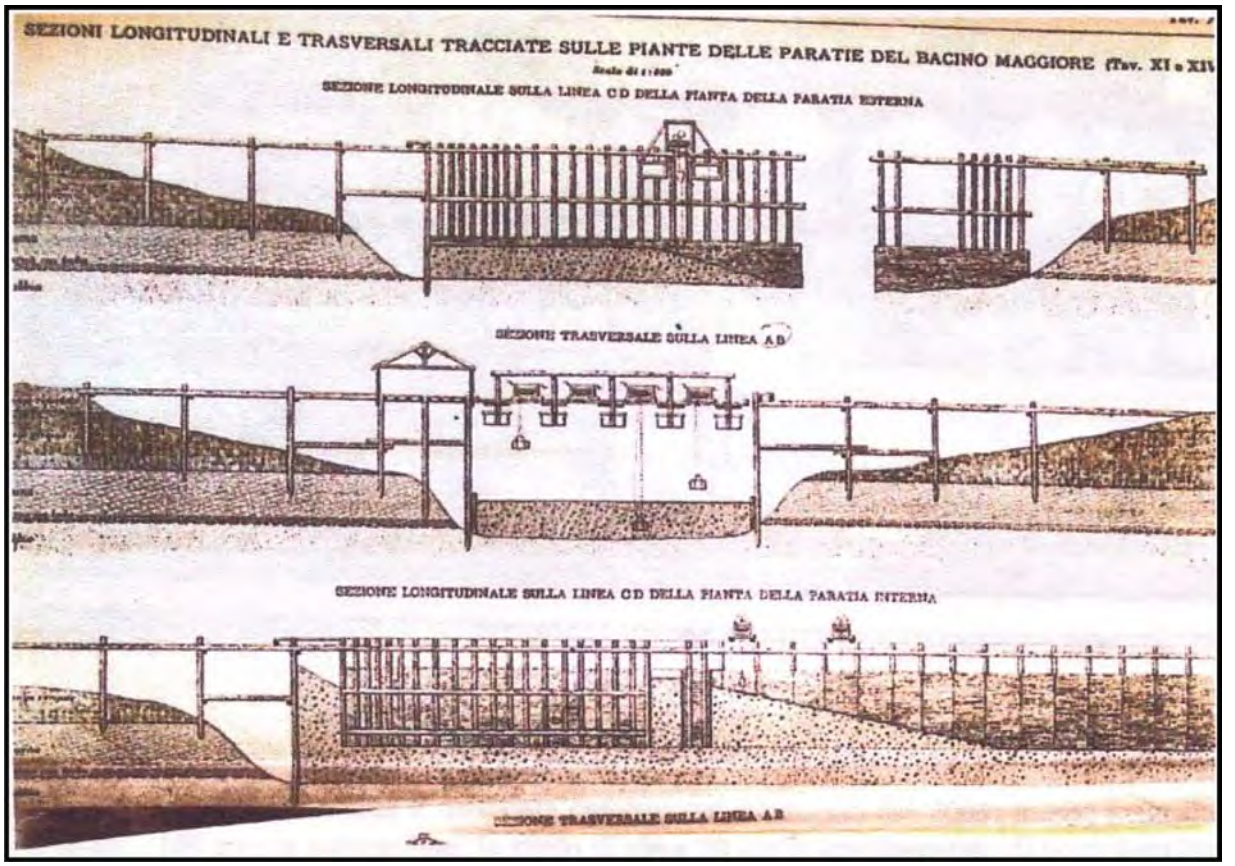

Fig. 2. Structural scheme of a dry dock and the provisional work necessary for the realization phase.

2.1. The construction technique

The dry dock in Messina was built by the "gravity" technique [1,2] and it is one of the first examples of this kind of structures in Italy. Unfortunately, the original documentation of the dry dock project, drawn up by the two chief engineers F. Damiani and G. Medici, went lost. The documentation, with the included references, can be partially recovered from the project of another similar dry dock built in the Venice shipyard few years later.

The available information has evidenced that the basin was dug following the open cut technique with excavation sides having a slope of about 45°. Moreover, explosives were used to cut the polygenic conglomerate (pudding) located at 0.6 m below the ground level.

The subsequent construction of the dry dock structure was probably carried out using a movable bridge equipped with overlapped lines to allow the movement of the trolleys used for conglomerate transportation (Fig. 2). Finally, filling material was used to fill up the hollow space between the sidewalls of the dock structure and the former rocks.

The sidewalls and the bed of the dry dock were built with pozzolanic material, sand and gravel aggregates, adding hydrated lime as a binder material.

3. Geological and geotechnical framing

3.1. Characterization of area

The area where the dry dock is located is characterized by a narrow peninsula which creates a protected natural dock for ships landing (Fig. 3). The deposits in the area were interested by different surveys, especially in the period September 2005 and July 2009, in order to get a precise characterization of the soil stratigraphy near the dry dock.

Fig. 3. Aerial view of Messina with the identification of the port (left) and of the dry dock within the port (right).

Table 1
Depth and SPT results.

drilling	depth [m]	N1 [/]	N2 [/]	N3 [/]	N_{spt} [/]
SS1	16.50	–	–	–	–
SS2	16.50	10	9	11	20
S1	19.00	–	–	–	–
S2	19.50	–	–	–	–
S3	14.50	6	6	6	12
S4	8.50	7	6	6	12
S5	19.50	–	–	–	–
S11	10.00	–	–	–	–
S12	13.00	–	–	–	–

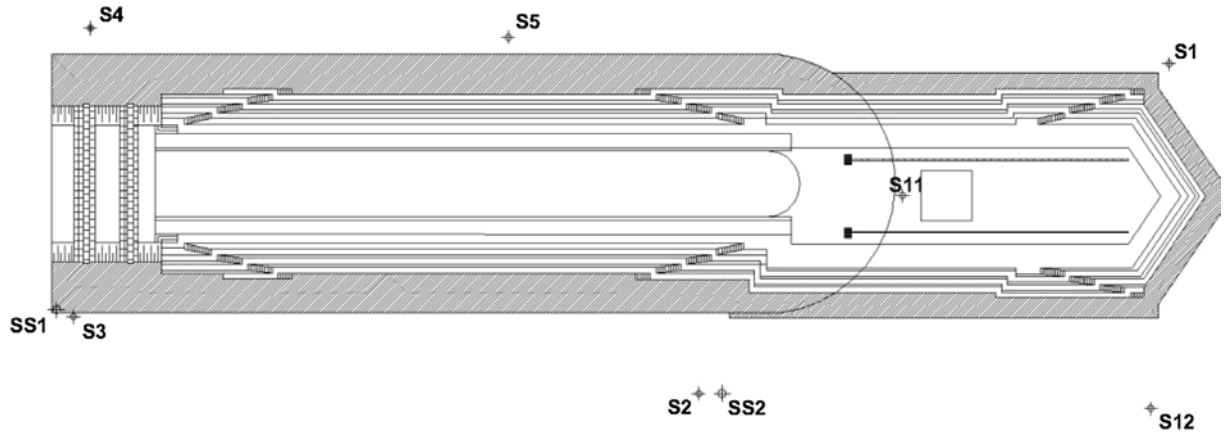

Fig. 4. Dry Dock plan with the SPT drillings points (S: 2005 tests, SS: 2009 tests).

3.2. Soil tests on site

The characterization of the soil around the dry dock was conducted by appropriate prospections carried out near the dock. With reference to the construction technique above described, the investigated area is approximately identified with the upper backfilling of the dry dock sidewalls.

In particular, geophysical prospections were performed in 2005 including:

- 2 electrical resistivity tomographies for 112.50 m total length, placed on the left side of the dry dock (respect to the sea), to evaluate the apparent resistivity;
- 1 seismic tomography, placed in the same area of the electrical tomography for a length of 85 m, in order to evaluate the seismic waves velocity;

Besides tomographies, 7 mud drillings (Table 1) were also made in order to determine the soil's stratigraphy (S1, S2, S5, S11 and S12 in Fig. 4) and to execute SPT tests (S3 and S4 in Fig. 4).

Table 2
Compression tests results on conglomerate.

drilling	Structural element	n° specimens	$f_{opera,m}$	f_{ck}
			[MPa]	[MPa]
CP1	Floor of "gargame"	3	9.00	2.58
CP2	Floor of old dock	3	6.50	N.D.
CP3	Floor of new dock	3	30.20	27.53
CP4	Old dock walls	3	41.20	40.48
CP5	New dock walls	3	16.70	11.65

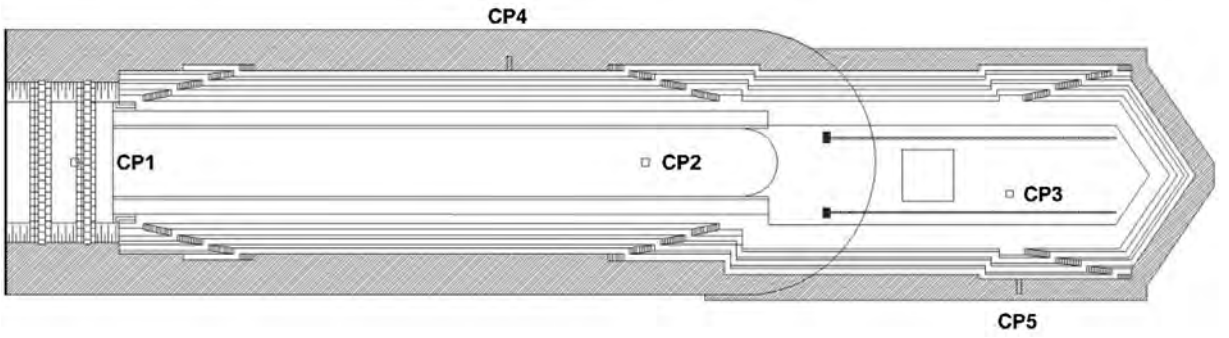

Fig. 5. Dry Dock plan with the points of the investigations.

In 2009, other geological, geophysical and geotechnical investigations were performed. In particular:

- 2 drillings near the loading dock (SS1) and another one on the right side of the dry dock (SS2, respect to the sea);
- 1 MASW on the floor of the dry dock for the acquisition of seismic profile.

The investigations around the dry dock have shown the sequence of three lithological units having different geomechanical characteristics, in particular:

- a backfill consisting of silty sands with gravels and anthropically reworked materials;
- fine sands and silts;
- gravels and coarse sands.

3.3. In situ conglomerate tests

The characterization of the dry dock's conglomerate was performed during the same period of the above mentioned soil investigations. In particular, 5 conglomerate core samples were taken and subsequently 15 specimens of conglomerate were extracted from these samples in order to be tested. The compression test results are shown in Table 2, while the investigation points (CP1 ÷ CP5) are identified in Fig. 5.

4. Numerical analysis

The analysis of the seismic behavior of the dry dock is carried out considering static and dynamic loads. Three finite element models representing both structure and soil ("structure + soil") are implemented referring to [3] about the modelling technique in terms of elements, mesh generation and construction stage analysis.

The three models implemented by MIDAS GTS software represent: the section AA of the old dry dock (called "*gargame area*"), the section BB of the old dry dock and the section CC of the new dry dock (Fig. 6).

The FEM of section AA is characterized by solid elements (only the ship-lock is represented by an equivalent plate element), whereas the models of the sections BB and CC are characterized by plane strain elements [4].

For each model, the boundary conditions are the following:

- vertical supports in the base nodes to restrain the vertical displacements;
- horizontal supports in the lateral nodes of the mesh to permit vertical soil settlements.

The section AA modelling with solid finite elements is necessary because it is the initial section of the dock; here the boundary conditions vary along the longitudinal axis due to the presence of the ship-lock (in fact, the pressure of the water

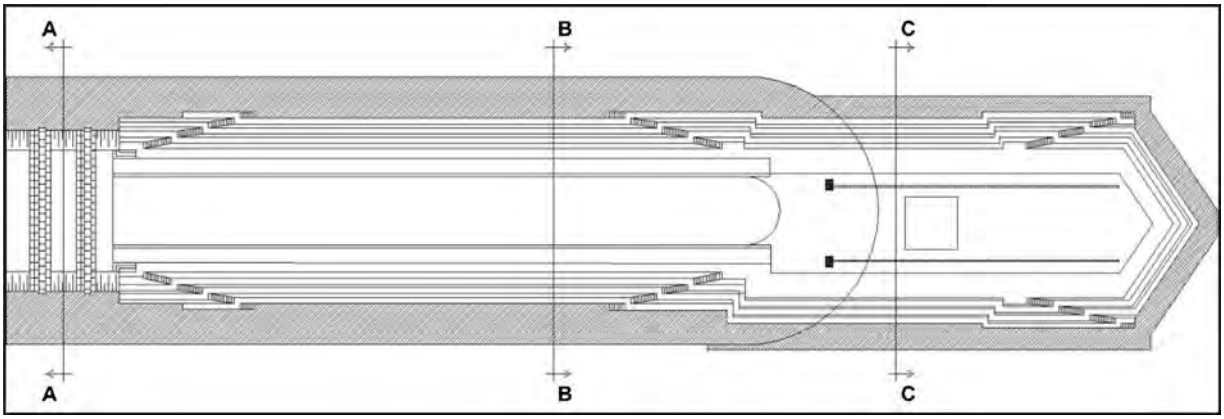

Fig. 6. Dry dock plan, with the sections analyzed by the finite element models.

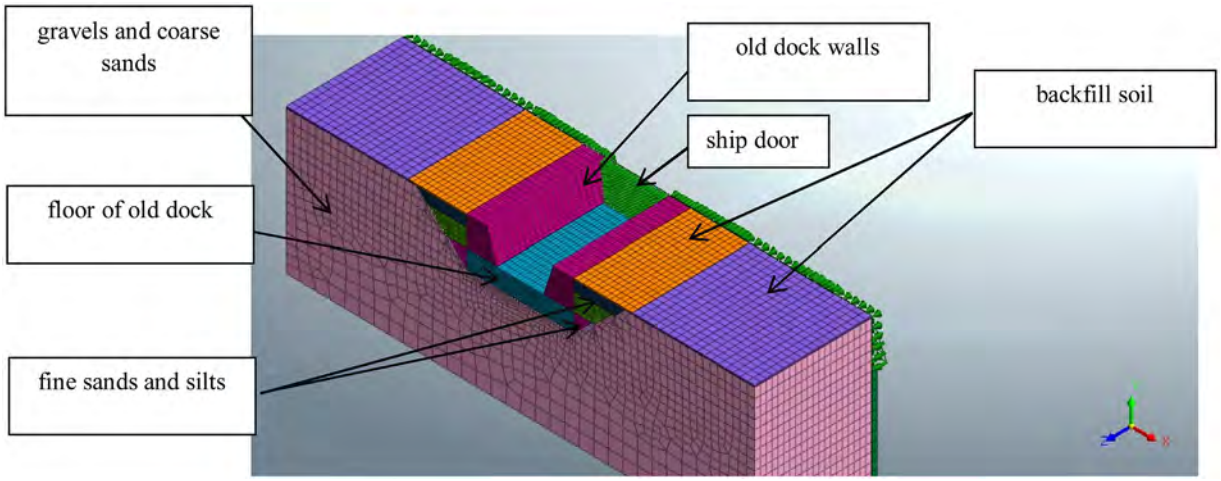

Fig. 7. Section AA, water pressure on the external side of the ship-lock.

acting on its external side has to be considered, Fig. 7). In the 3D FEM of section AA a total width of 50 m has been considered in order to take into account the influence of the soil boundary conditions on the gargame section.

Referring to the solid FEM, it is important to specify that in section AA, namely "*gargame area*", there is the entrance of the dry dock. This section (Fig. 8) is characterized by the absence of a backing arch, generally present in other dry docks (i.e. in La Spezia dry dock). The absence of the backing arch causes higher values of stresses in the foundation slab with respect to usual configurations. This geometry causes severe swellings under the threshold of the basin. To temporarily solve this problem, a number of concrete blocks have been positioned on the foundation. Moreover, the zone close to the section AA has been reinforced by applying steel plates anchored with ties to the sides of the dry dock. In the FEM, the concrete blocks are not modeled but their self-weight effect is represented by an equivalent pressure whereas the steel plates are not implemented because the aim of the FEM is to investigate mainly the stresses field in the foundation. The modelling of the steel plates could be more useful if the aim of the analysis would be the evaluation of the stresses in the side walls, where actually important cracks were not detected.

Referring to the FEM implemented by plane elements, it is important to specify:

- in section BB ("old dry dock") there are the above mentioned drainage tunnels (Fig. 9);
- section CC ("new dry dock", Fig. 10), regarding the dry dock lengthening carried out in the fifties of the last century, is characterized by a foundation mat with a concave upward shape in the extrados and by the absence of the drainage tunnels.

4.1. Loads

4.1.1. Static loads

The loads considered in the analysis are described in the following:

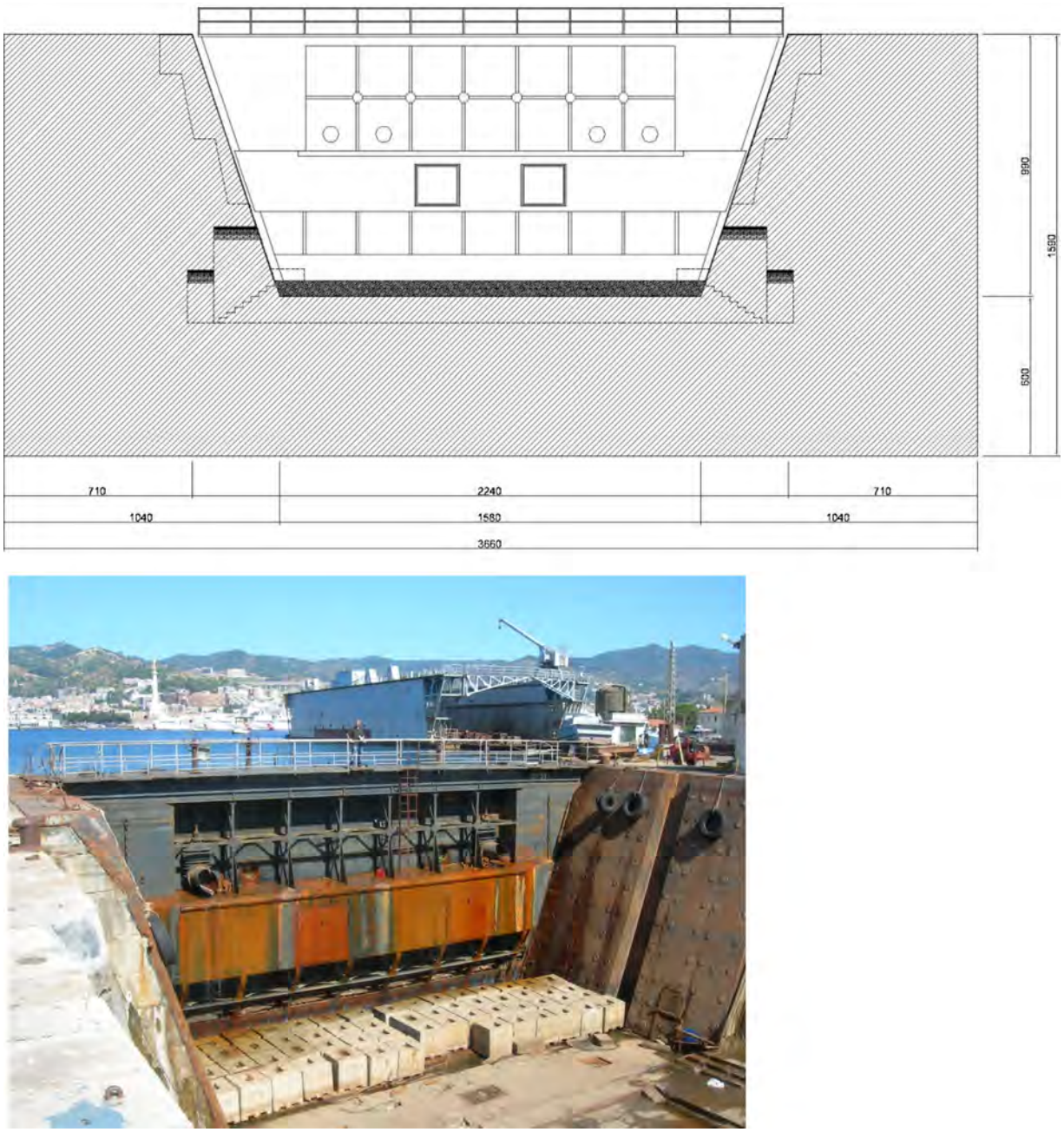

Fig. 8. Section AA, named "gargame area" – dimensions and photo.

- dead load on the square equal to 40 kN/m^2, applied in each section, due to sheds and structures present beside the dry dock together with the weight of the material used during maintenance of ships (Fig. 11, Fig. 12 and Fig. 13), almost always present during the year;
- load on the right side (respect to the sea) due to a crane moving on tracks (132.00 m length, 6.00 m gauge, 12.00 m race starting from front bulkhead, Fig. 11). The load (30 kN/m^2) is evaluated according to the drawings of the supplier;
- dead load due to presence of the ship inside the basin; it is represented by a static pressure distributed over the entire length of the dry dock. This load is transmitted on the foundation floor of the basin by the docking blocks, 1.00 m large each one (Fig. 14). On each docking block, a dead load of 135 kN is applied, owing to the weight of the ship. Considering 3 docking blocks per cross section, the total ship load in the generic section of the basin is about 400 kN;
- seismic load, considering both the structure and ship masses;

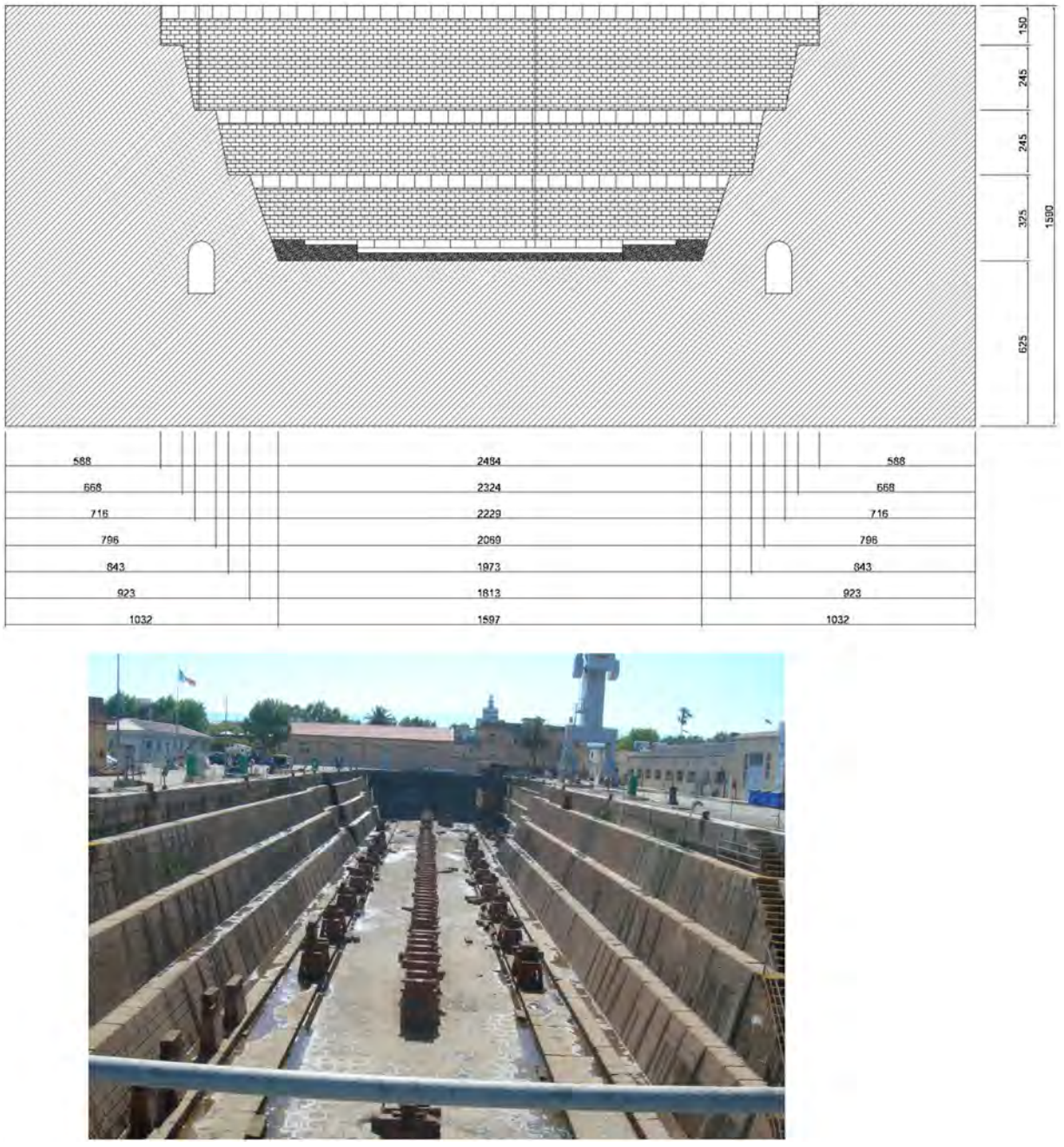

Fig. 9. Section BB, named "old dry dock" – dimensions and photo.

- load due to the presence of counterweight concrete blocks in the mentioned *gargame area*. In the FEMs, the concrete blocks are modeled as an equivalent (in terms of weight) uniform pressure load. For each block, a specific weight of 23 kN/m^3 is considered, while the height of the stack of blocks is 1.00 m. It must be underlined that this load is applied only to evaluate the improvement of operational conditions and to evaluate the possible mitigation of swelling problems near the ship-door (as described above for the AA section).

In addition, an aquifer located approximately 1.00 m depth underground (with respect to the floor of the wharf) was also considered.

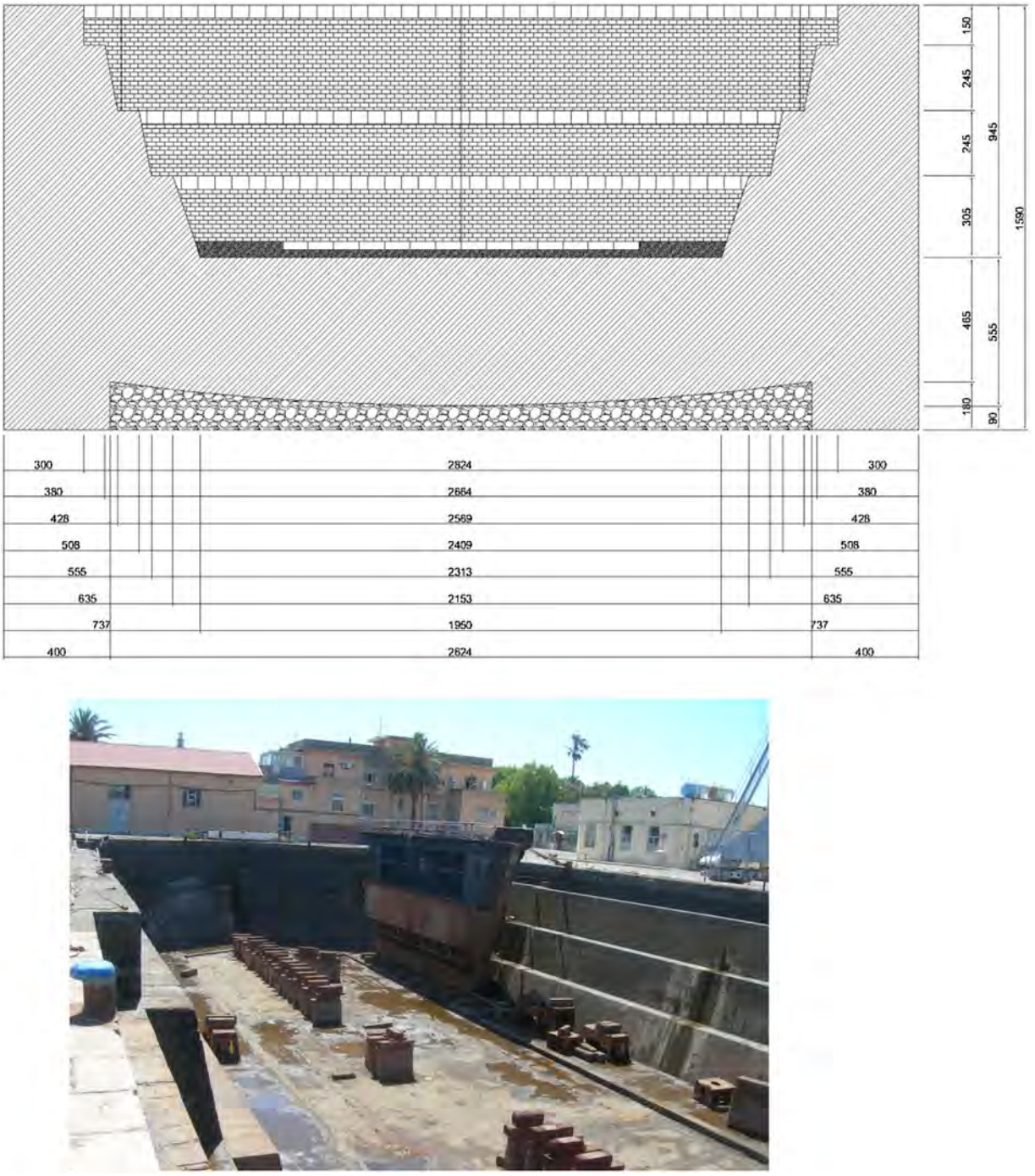

Fig. 10. Section CC, named "new dry dock" – dimensions and photo.

4.1.2. Seismic action

In Ref. [12], the seismic action depends on the intrinsic characteristics of the structure and its strategic importance in relation to the intended use. Whereas the strategic importance of the present structure regards either the military and the civil contests, the site spectrum (Fig. 15) is defined by the parameters of Table 3 referring to the Collapse Limit State (SLC). The response spectrum is defined in order to generate the set of accelerograms adopted to represent the seismic input in the FEMs.

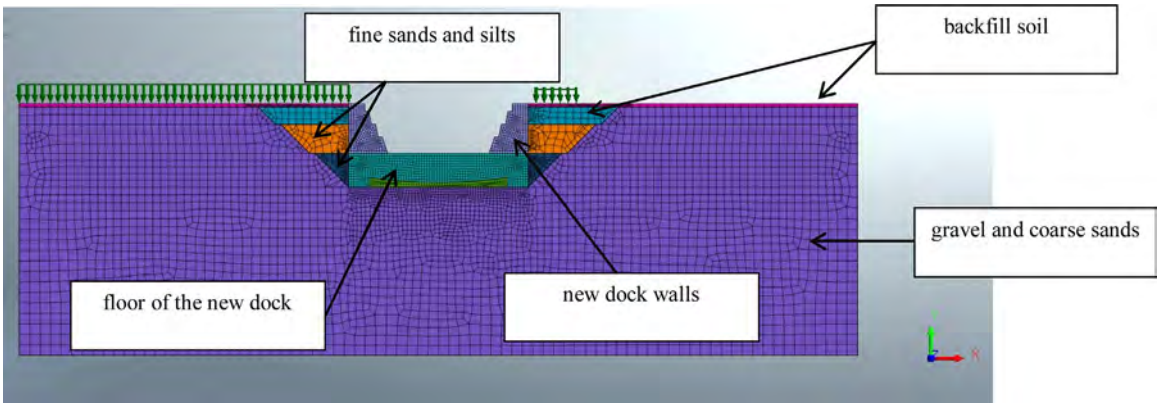

Fig. 11. load on the square (left) and crane load (right) in the 2D-FEM of Section CC.

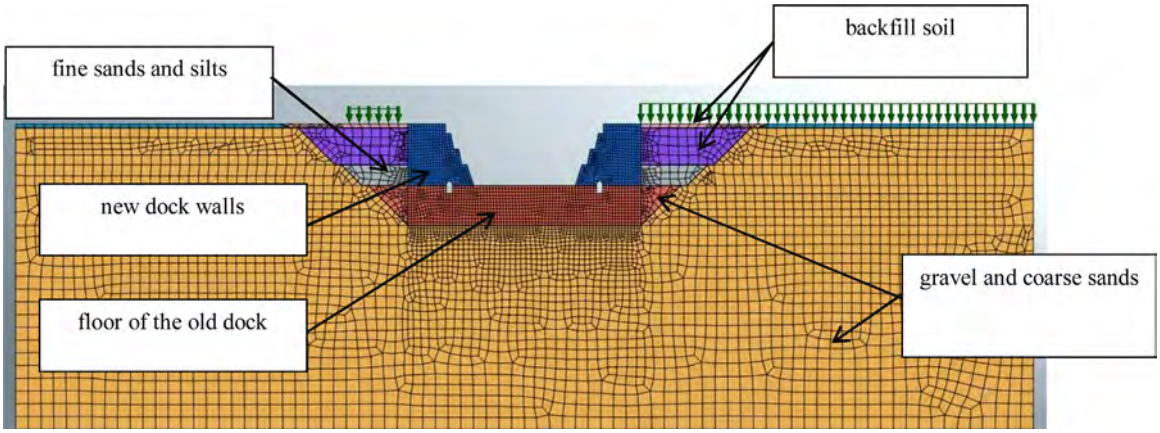

Fig. 12. load on the square (left) and crane load (right) in the 2D-FEM of Section BB.

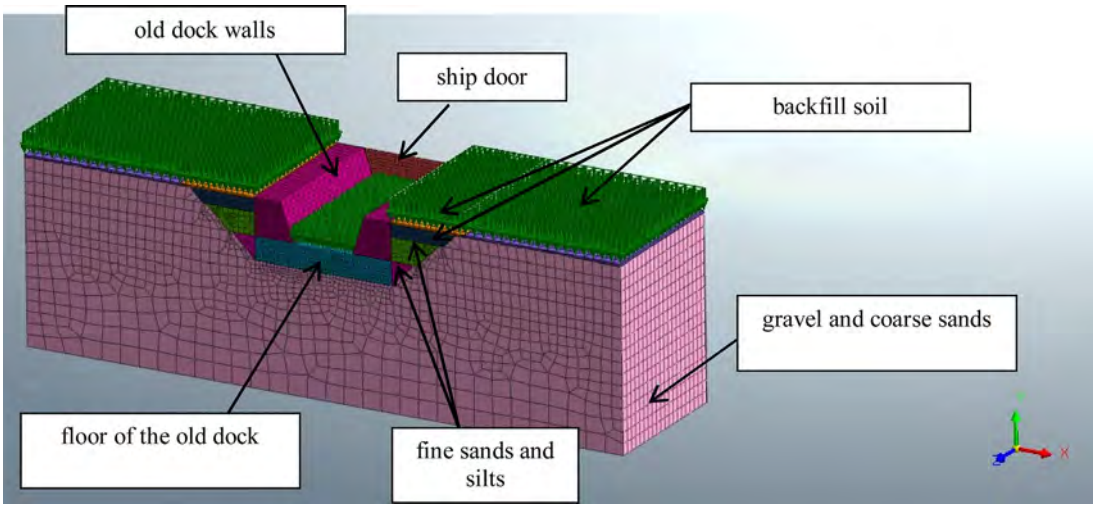

Fig. 13. load on the square and concrete blocks equivalent load in the 3D-FEM of section AA.

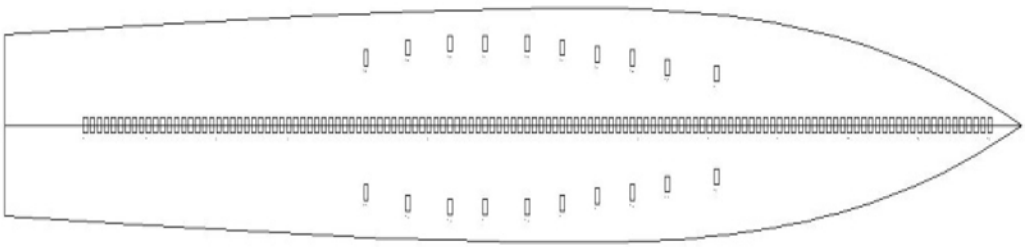

Fig. 14. Example of docking blocks arrangement.

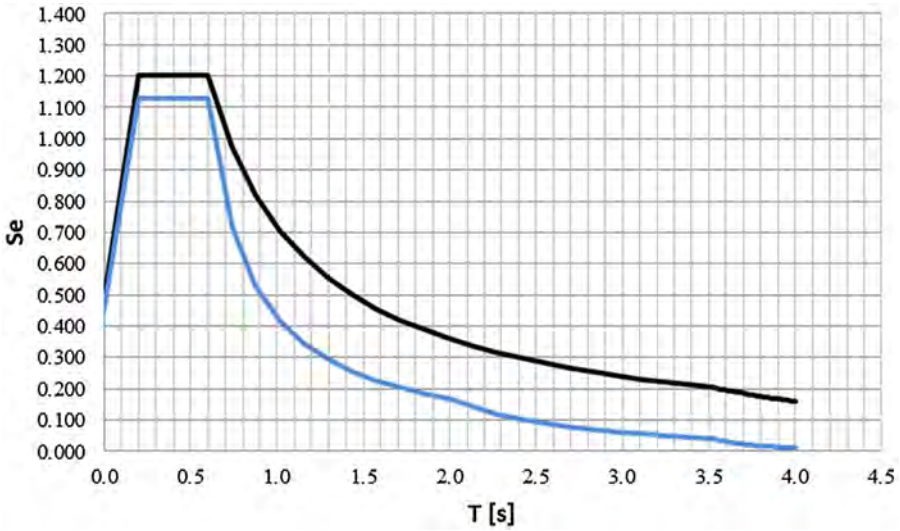

Fig. 15. Response spectrum for the vertical (in blue) and horizontal (in black) components.

Table 3
Response spectrum parameters.

Limit state	SLC		
Life of the structure	V_N	[year]	≥100
Class of the use's category	[/]	[/]	III
Coefficient for the construction's use	C_u	[/]	1.5
Return Period	V_R	[/]	150
Expentacy	P_{VR}	[%]	5
Topographic coefficient	S_t	[/]	1.00
Stratigraphic coefficient	S_s	[/]	0.92
Site acceleration	a_g	[1/g]	0.485
Maximum acceleration	a_{max}	[1/g]	0.446
Global ductility factor	q	[/]	1

Referring to the previous Fig. 15, the equations defining the four branches of the horizontal component of the elastic response spectrum are listed below:

$$0 \le T \le T_B \quad S_e(T) = a_g \cdot S \cdot \eta \cdot F_0 \left[\frac{T}{T_B} + \frac{1}{\eta \cdot F_0}\left(1 - \frac{T}{T_B}\right)\right]$$
$$T_B \le T \le T_C \quad S_e(T) = a_g \cdot S \cdot \eta \cdot F_0$$
$$T_C \le T \le T_D \quad S_e(T) = a_g \cdot S \cdot \eta \cdot F_0 \left[\frac{T_C}{T}\right]$$
$$T_D \le T \quad S_e(T) = a_g \cdot S \cdot \eta \cdot F_0 \left[\frac{T_C \cdot T_D}{T^2}\right]$$

where:

- $S_e(T)$ is the vertical Cartesian coordinate of the horizontal elastic response spectrum;
- T is the vibration period of the structure;

Table 4
Combination coefficients for the static loads considered in the seismic analysis.

Static loads (referring to paragraph 4.1)	Section AA	Section BB	Section CC
Load on the square (dead load type)	1	1	1
Crane load (dead load type)	0	1	1
Ship (live load type)	0	1	1
Concrete blocks (dead load type)	1	0	0

- a_g is the design ground acceleration, for the considered site, on type A ground;
- S is a coefficient taking into account the type of soil and topographic conditions of the site; its value is given by the relation $S = S_S \cdot S_T$ where S_S is the stratigraphic amplification coefficient and S_T is the topographic amplification coefficient;
- T_B, T_C, T_D are the periods limiting the various branches of the function describing the spectrum;
- η is a coefficient taking into account the conventional viscous damping different from $\xi = 5\%$, its value is given by the equation $\eta = [10/(5+\xi)]^{1/2}$;
- F_o is the magnification factor for the considered site, $F_o = 2.491$.

The mentioned limiting periods of the spectrum depend by the reference period T_C^* which takes into account the soil characteristics of the considered site (in this case $T_c^* = 0.432$ s). In particular:

- $T_C = C_c \cdot T_C^*$, is the upper limit of the period of the constant spectral acceleration branch (in this case $T_C = 0.598$ s);
- $T_B = T_C/3$, is the lower limit of the period of the constant spectral acceleration branch (in this case $T_B = 0.199$);
- $T_D = 4.0 + (a_g/g) + 1.6$, is the value defining the beginning of the constant displacement response range of the spectrum (in this case $T_D = 3.530$).

Moreover, even referring to the previous Fig. 15, the relations to define the vertical component of the elastic response spectrum are:

$$
\begin{aligned}
&0 \le T \le T_B \quad && S_{ve}(T) = a_g \cdot S \cdot \eta \cdot F_V \cdot \left[\frac{T}{T_B} + \frac{1}{\eta \cdot F_V}\left(1 - \frac{T}{T_B}\right)\right] \\
&T_B \le T \le T_C \quad && S_{ve}(T) = a_g \cdot S \cdot \eta \cdot F_V \\
&T_C \le T \le T_D \quad && S_{ve}(T) = a_g \cdot S \cdot \eta \cdot F_V \cdot \left[\frac{T_C}{T}\right] \\
&T_D \le T \quad && S_{ve}(T) = a_g \cdot S \cdot \eta \cdot F_V \cdot \left[\frac{T_C \cdot T_D}{T^2}\right]
\end{aligned}
$$

where the same above mentioned symbols are used (here $S_{Ve}(T)$ represents the vertical Cartesian coordinate of the vertical elastic response spectrum and F_v the vertical magnification factor for the considered site). In this case: $T_C = 0.150$ s, $T_B = 0.050$ s, $T_D = 1$ s and $F_V = 2.336$.

Once the response spectra are defined, the seismic analysis in the FEMs is carried out by performing a "step by step" analysis, through direct integration of the motion's equations in the time domain and considering a 20 s ground acceleration (corresponding to the complete duration of the ground motion). Thus, the seismic action is represented by a set of accelerograms acting in both horizontal and vertical directions (Fig. 16); all of these accelerograms must be compatible to the above defined site response spectrum.

Consequently, the seismic action considered for each structural analysis is represented by three different accelerograms applied along the three principal directions of the coordinate system (two in the horizontal plane and the vertical one). By the use of several set of such accelerograms and the repetitions of the integration of the motion equations, the 3D state of stresses in the soils and structure can be evaluated in an appropriate manner. The artificial spectrum-compatible accelerograms are generated by means of the SIMQKE_GR software [13], developed by the University of Brescia (Italy).

Therefore, for each considered section (AA, BB and CC), the structural results in terms of stresses and deformations can be determined by considering the static and seismic loads applied on the "structure + soil" finite element model (FEMs). In each FEM (representing one of the three sections AA, BB and CC), the above mentioned static loads are considered. In order to reproduce the actual static situation, all the static loading conditions are combined considering a partial factor equal to 1 ($\gamma_F = 1$ for each type of static loads, if present, Table 4). Once the structural results under static loads are determined, the seismic action is applied on the "structure + soil" finite element models (FEMs) by a set of artificially-compatible spectrum accelerograms and the consequent step by step time history analysis is carried out on the three models: with the soils represented by solid elements for the section AA and by plane strain elements for the sections BB and CC.

Preliminarily, in order to evaluate the dynamic behaviors of sections AA, BB and CC (old and new dry docks) [9], three eigenvalue analyses were carried out on the three finite element models in order to evaluate, for each section, the natural periods and mode shapes of the new and old dry docks.

The structural damping is then evaluated by the Mass and Stiffness Proportional Method [11] on the basis of the first and second natural periods. The damping ratio is assumed equal to 5% for these two modes.

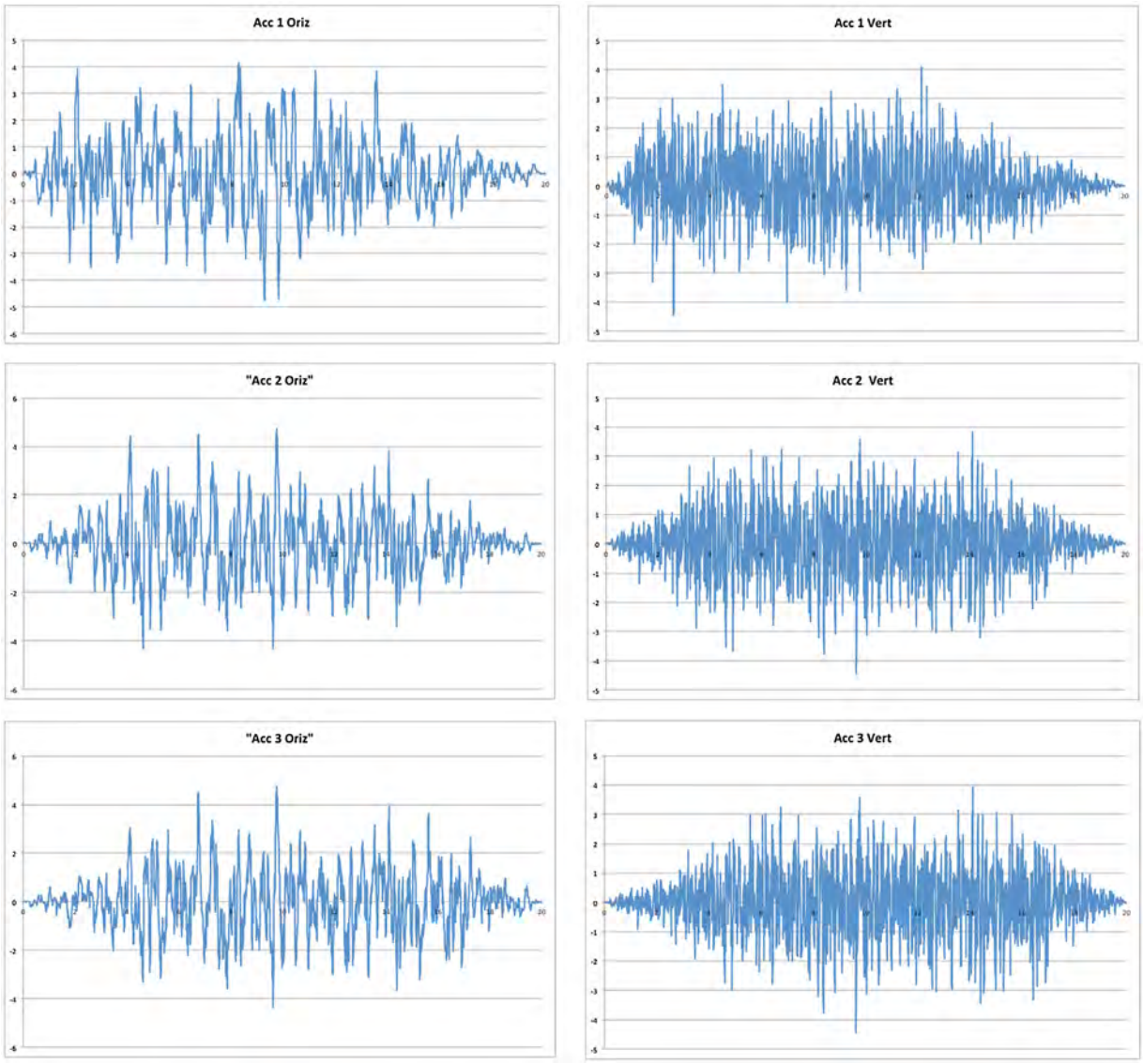

Fig. 16. Ground motions for "step by step" analysis. The accelerations are expressed in m/s^2 while the time is reported in s.

Finally, in order to evaluate the effects of the presence of the ship in maintenance condition in the dry dock basin, only in the previous 2D models (sections BB and CC, the only ones interested by the ship), the ship is modeled (in a simplified way) with a nodal mass concentrated in the ship's center of gravity. This equivalent nodal mass is connected to the docking blocks by means of rigid links while the blocks are represented by elastic links fixed to the dock floor (Fig. 17).

4.2. Definition of mechanical properties of ground and conglomerates

4.2.1. Static analysis

Geological studies and investigations have led to the definition of the geo-mechanical characteristics of the soils to be used in the numerical analysis. In the following, a summary of these characteristics is reported in Table 5. Moreover, in Table 6, the different typologies of soils adopted to implement the models of the mentioned sections AA, BB and CC are identified.

The mechanical properties [5] of the conglomerate, adopted in the numerical analysis, are obtained from the previous mentioned tests on core samples and are summarized in Table 7.

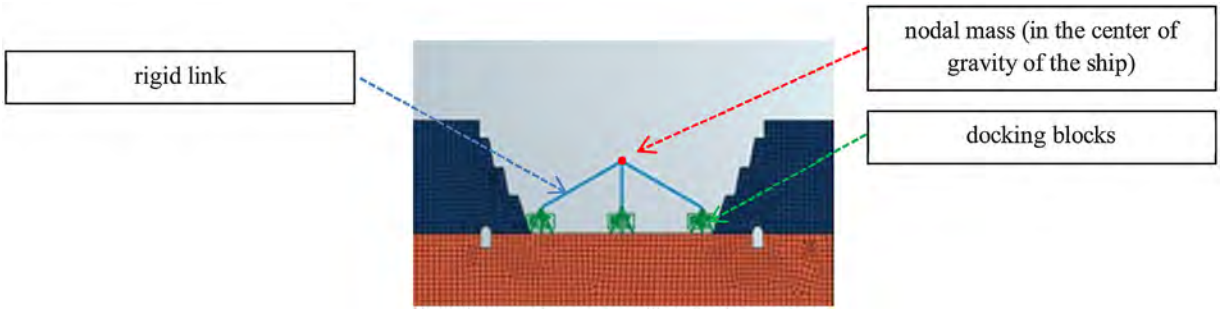

Fig. 17. Detail of the ship implementation (Section BB).

Table 5
Geo-mechanical specifications of soils around dry dock before and the implementation (γ = weight density; ϕ = friction angle, c = cohesion).

Soil Type		γ [kN/m^3]	ϕ [°]	c [kN/m^3]	E [MPa]	ν [/]
Before the construction	Polygenic conglomerate "pudding"	17	45	350	250	0.08
After the construction	Backfill	14	22	0	2	0.3
	Fine sands and silts	16	30	0	5.25	0. 3
	Gravels and coarse sands	18	33	0	34.7	0.3

Table 6
Soil typologies in the different sections (after the dry dock construction).

Soil Types	*Section AA*	*Section BB*	*Section CC*
Backfill	from 0.00 to − 3.95 m	from to 0.00 m to −6.40 m	from 0.00 to −3.95 m
Fine sands and silts	from − 3.95 m to −15.90 m	from −6.40 m to −9.65 m	from −3.95 m to −15.90 m
Gravels and coarse sands	under	from −9.65 m to −15.9 m	under

Table 7
Mechanical properties of the dry dock conglomerates.

Conglomerates types	γ [kN/m^3]	E [MPa]	ν [/]
Floor of old dock	18	10000	0.10
Floor of new dock	24	32000	0.15
Old dock walls	23	39000	0.15
New dock walls	22	21000	0.15

4.2.2. Dynamic analysis

The seismic characterization of the soils [10] around the dry dock was performed considering the modulus of elasticity and the shear modulus [6], according to Ohta et al. (1978) equation [7], where the correlation between the shear wave velocity (V_s) and the result of Standard penetration tests (SPT) is described by the following expression:

$$V_s = C \cdot (N_{60})^{0,17} \cdot (z)^{0,2} \cdot f_a \cdot f_g \quad [\mathrm{m/s}]$$

where:

- C = 68.5
- $N_{60} = N_{spt} \cdot (ER/60)$; ER/60 = 1.08; N_{60} = SPT number of blows normalized respecting 60% efficiency;
- z = depth [m];
- f_a, f_g = corrective factor taking into account the age and the influence of the deformation's rate.

By the shear wave velocity, it is possible to calculate the shear modulus G and the modulus of elasticity E for dynamic conditions, by the following equations [8]:

$$G = \gamma \cdot V_s^2 \quad [\mathrm{MPa}]$$

$$E_d = 2 \cdot G \cdot (1 + \nu) \quad [\mathrm{MPa}]$$

where:

Table 8
Shear modulus (G), shear deformation lowering modulus (G/3), modulus of elasticity (E) for soils adopted in the seismic analysis.

Soil Type	G	G/3	E
	[MPa]	[MPa]	[MPa]
Conglomerate	849	283	736
Gravel	90	30	78
Sand	55	18	37
Backfill after excavation	41	14	27
Backfill before excavation	16	5	14

Table 9
Shear wave velocity (Vs), shear modulus (G), shear deformation lowering modulus (G/3) and modulus of elasticity (E) of conglomerates adopted in the seismic analysis.

Conglomerate Type	V_s	G	G/3	E
	[m/s]	[MPa]	[MPa]	[MPa]
Floor of old dock	3000	16514	5505	12110
Floor of new dock	3000	22018	7339	16881
Old dock walls	3000	21101	7034	16177
New dock walls	3000	20183	6728	15474

- γ = total unit weight;
- V_s = shear wave velocity;
- ν = Poisson's ratio.

In the present case, the most representative values for the different kind of soils are reported in Table 8.

For the characterization of the structural conglomerates, the value of the shear wave velocity was equal to 3000 m/s, according to the average compacted concrete case. The most representative mechanical properties for the different kind of conglomerates are listed in Table 9.

4.3. Results

4.3.1. Static analysis

The static analysis carried out by the application of all the before mentioned vertical loads (obviously without considering the earthquake) has pointed out the characteristic behavior of the dry dock's structure: it appears similar to a double supporting wall under water-bed. In Ref. [14] a method to calculate the wall under water-bed is given.

The structural conditions of the dry dock under the considered static loads are determined by performing a construction stage analysis [15], taking into account all the main phases historically involved in the construction of the dry dock (the influence of the excavation phases on the stress fields of a generic soil volume can be found in Ref. [16]). The sequence of the construction phases considered in the analysis (Fig. 18) is summarized as follow:

- starting conditions;
- starting excavation;
- ending excavation;
- foundation floor execution;
- walls construction;
- backfilling;
- ship placement.

In the last stage of the analysis, the presence of the in-maintenance ship is represented by a rigid structure supported on the actually used three lines of docking blocks placed on the bed of the dry dock. In each phase, the level of the ground water varies according to the excavation steps. Initially (at the first stage) the quote of the ground water is considered at −1.00 m from the wharf. Finally, in the last stage, the level of the ground water is brought again at −1.00 m from the wharf, like it was in the first stage. The variation of the ground water level is implemented for each stage of the FEM by assigning the related quotes and is provided because the pressure due to the water on the lower surface of the bed mat could cause tensile stresses in the conglomerate, which is characterized by a very low tensile strength. For example, as it will be described for section AA, the structural effects due to the pressure of the ground water are obviated by positioning some concrete blocks (working as counterweights). The considered load combinations are the same for the BB and CC sections.

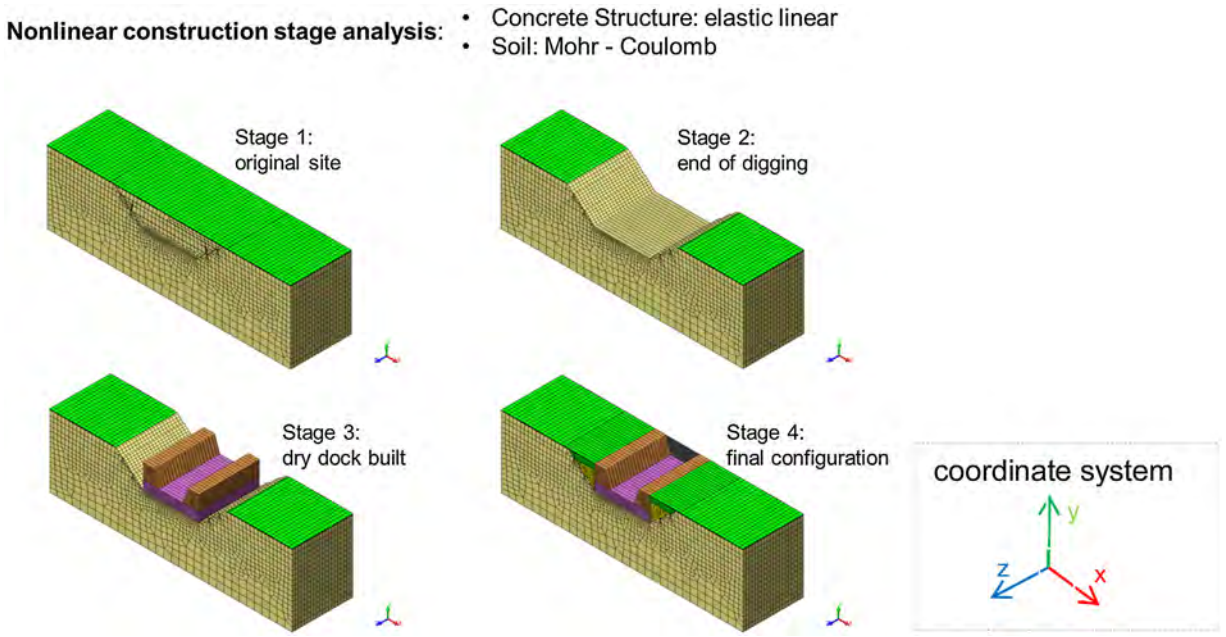

Fig. 18. Construction stage analysis.

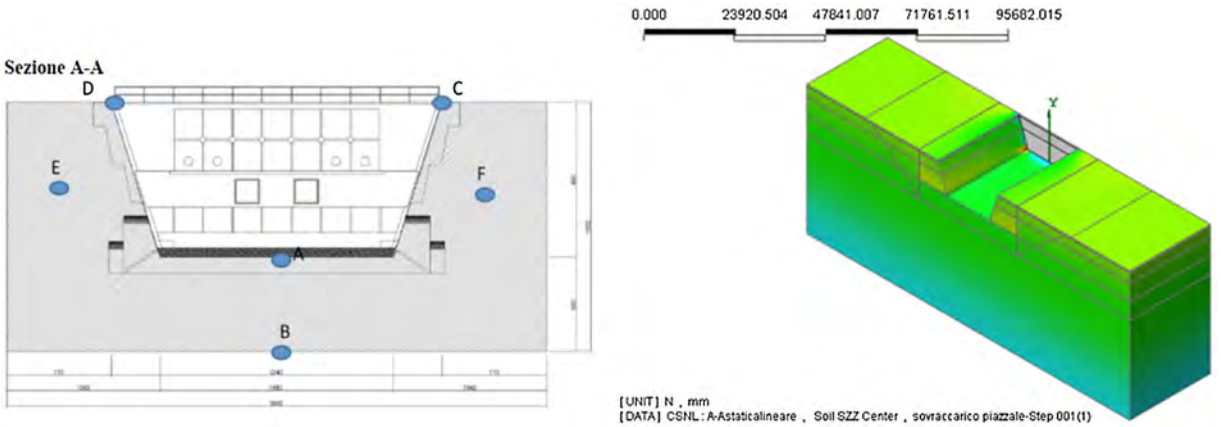

Fig. 19. Section AA, with the main points analyzed and related FEM.

4.4. AA section—"gargame area"

The implementation of the 3D model (by using solid finite elements) has regarded the section AA, also called "gargame area" (Fig. 19).

Known the geometry and the values of the static loads, the results are obtained in terms of stresses and displacements (see Table 10). The obtained stresses show that the bending of the bed mat causes tensile stresses of about 0.3 MPa in the longitudinal direction of the dry dock (the "z" axis) at point "A". This value is very close to the tensile strength of the mat pozzolanic conglomerate. The loading condition considered in this analysis do not consider the presence of the ship because, in the daily use of the dry dock, this area is clear.

At point "B", the evaluation of the stresses at the intrados of the bed mat shows a very low compression.

Regarding the stresses in horizontal direction (transversally with respect to the dry dock, axis x) they are characterized by low compression values, like it happens in the old dry dock (see the next section).

In conclusion, despite most of the volume of conglomerate in this area of the dry dock is subjected to widely acceptable compression stresses, near the point A of the gargame area slab the tensile stresses are close to the conglomerate's tensile strength following in a very damaged status of the slab; for this reason, some concrete blocks have been used to stabilize the bulge of the foundation mat, working as counterweights.

Table 10
Static analysis: displacements and stress values at the main points of section AA ("gargame area").

Points	without blocks					
	Dx [mm]	Dy [mm]	Dz [mm]	σxx [MPa]	σyy [MPa]	σzz [MPa]
A	−0.089	−1.022	7.255	0.310	−0.277	−0.577
B	−0.094	−2.830	0.040	−0.367	−0.314	−0.207
C	0.450	−6.541	2.249	0.246	−0.041	−0.415
D	−0.898	−6.243	2.250	0.246	−0.040	−0.407
E	0.950	−8.840	4.927	−0.514	−0.145	−0.045
F	−1.264	−9.215	4.927	−0.045	−0.143	−0.045

Note: displacements: the negative values represent a downwards displacements; stresses: the negative values represent compression stresses.

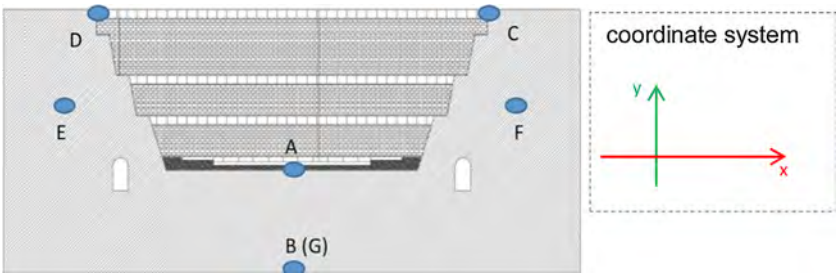

Fig. 20. Section BB, named old dry dock with the main points analyzed.

Table 11
Static analysis: displacements and stress values valued at the main point of section BB ("old dry dock").

Points	Dx [mm]	Dy [mm]	σxx [MPa]	σyy [MPa]
without ship				
A	0.0	−3.6	−0.285	−0.00470
B	0.0	−4.5	−0.424	−0.1547
C	1.3	4.0	0.0005	−0.00660
D	−1.0	4.3	0.0002	−0.0070
E	−0.5	7.5	−0.0545	−0.1046
F	0.7	7.1	−0.0579	−0.1547
G	0.0	2.8	0.0471	−0.00250
with ship				
A	0.0	−10.4	−0.8714	−0.399
B	0.0	−11.2	0.0670	−0.230
C	−0.9	−1.3	0.0005	−0.0065
D	1.2	−1.0	0.0002	−0.0069
E	0.8	2.5	−0.0513	−0.1153
F	−0.7	2.1	−0.0528	−0.1134

Note: displacements: the negative values represent a downwards displacements; stresses: the negative values represent compression stresses.

The problematic status of tensile stresses does not occur on the shoulders of the dry dock where, in the recent years, some reinforcements has been applied by the use of steel plates anchored with ties to the structure.

4.4.1. Section BB—"old dry dock"

As before shown, the section BB called old dry dock is characterized by the presence of two drainage galleries. The Fig. 20 shows the section BB and in particular the points where the displacements and the stresses are evaluated by the FEM. The obtained values are listed in Table 11.

The analysis of the results in Table 11 shows that, in the condition without both the water inside the dock and the ship, but considering the lifting force exerted by the aquifer and the crane, the section BB is afflicted by deformations generating compression stresses either at the intrados and extrados in the bed mat. The compression values are very different themselves; it means that in the section BB there is a kinematic state tending to cause the "opening" of the dry dock and "dismissing" the points "C" and "D".

Referring to the previous Fig. 20, the point B refers to the extrados of the dry dock mat and it is topologically coincident with the point G but the displacements are here evaluated for different construction stages: the displacement at point G refers to the end of the excavation (before the bed mat realization), while the displacement at point B refers to the end of the construction process.

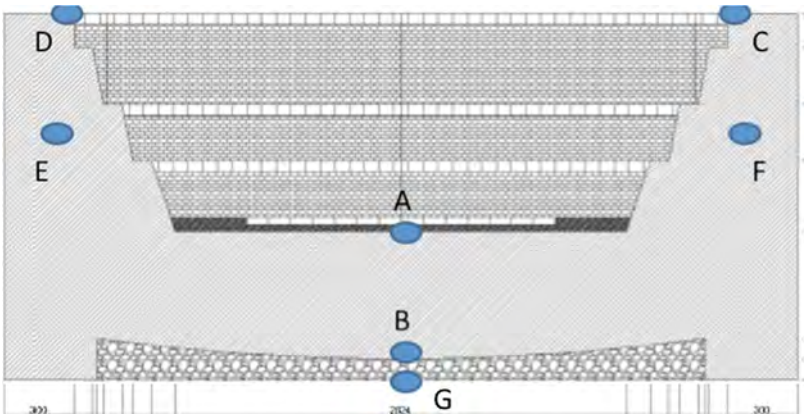

Fig. 21. Section CC "new dry-dock" with the main points analyzed.

Table 12
Static analysis: displacements and stress values valued at the main point of section CC ("new dry dock").

Points	Dx [mm]	Dy [mm]	σxx [MPa]	σyy [MPa]
without ship				
A	0.0	−8.6	−1.2567	−0.4016
B	0.0	−8.5	0.1798	−0.2217
C	−0.3	6.2	0.0016	−0.0045
D	0.5	6.6	0.0012	−0.0050
E	0.3	6.6	−0.577	−0.0975
F	−0.2	6.2	−0.606	−0.0999
G	0.0	3.1	0.5212	−0.00251
with ship				
A	0.0	−28.6	0.445	−0.00610
B	0.0	−28.5	−0.586	−0.17548
C	2.1	−15.3	0.00332	−0.00227
D	−1.9	−14.9	0.00293	−0.00282
E	−0.9	−15.0	0.00074	−0.14628
F	1.0	−15.4	−0.00203	−0.13587

Note: displacements: the negative values represent a downwards displacements; stresses: the negative values represent compression stresses.

Even if the condition with the simultaneous presence of the ship and all the vertical loads is considered, a rebalancing of the mentioned kinematic mechanism is verified with 10 mm subsidence displacements at point A.

The numerical analysis clearly demonstrates that the conglomerate of this section is interested by punctual and low tensile stresses.

4.4.2. Section CC—"new dry dock"

As before shown, the section CC called new dry dock is characterized by the absence of the drainage galleries; this section presents at the extrados a curved shape with an upward concavity. The Fig. 21 shows the section CC and the points where the displacements and stresses are evaluated by the FEM. These values are listed in Table 12.

Referring to the previous Fig. 21, the point B is placed at the extrados of the dry dock mat and it is not coincident with point G which refers to the end of the excavation process, before the bed mat was realized. Thus, in section CC (Fig. 21), the points B and G are not topologically coincident, differently with respect to Fig. 20 referring to the Section BB (old dry dock).

The results in the previous Table 12, obtained in the loading condition without the presence of both the water and the ship inside the basin, show that the deformations of the dry dock produce compression stresses at the extrados and tensile stresses at the intrados. In this situation, a kinematic behavior in which an "opening" of the dry dock can be recognized, causing displacements of the points "C" and "D" in the opposite direction themselves.

The stresses in this section show greater values than the previously calculated values in the corresponding section BB. In fact, a lot of cracks appear either on the bottom slab or on the vertical walls. The cracks in the vertical walls are directed from the top to the base mat; that means the presence of differential displacements around the interface region between the two different sections BB and CC.

Considering the loading condition with the simultaneous presence of the ship together with all the other vertical loads, a re-balancing of the mentioned kinematic behavior is verified, with an (about) 20 mm subsidence displacement.

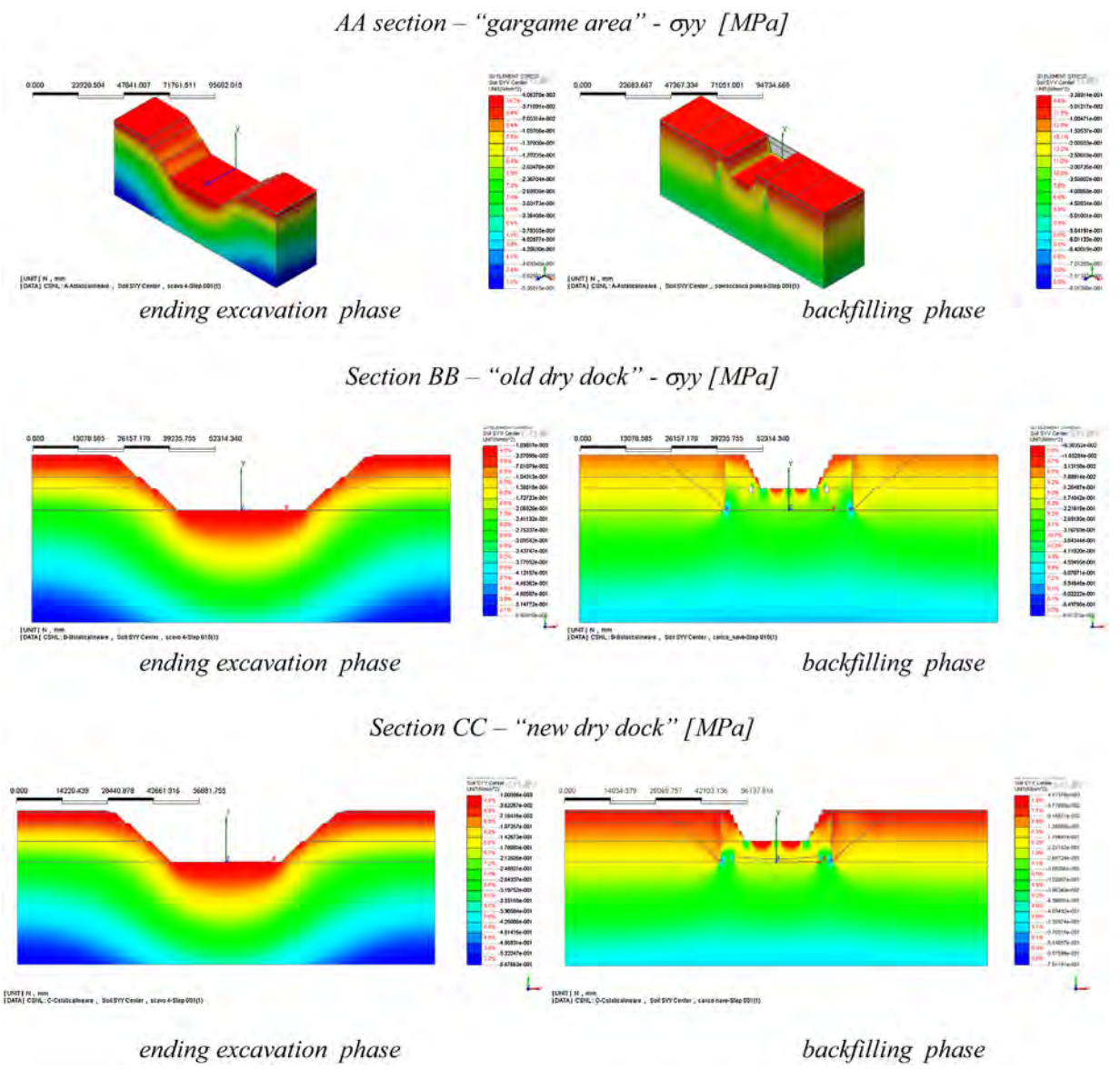

Fig. 22. σyy [MPa] in the sections AA, BB and CC for the phases "ending excavation" and "backfilling".

Analyzing the previous Tables 11 and 12, the different displacements and stresses between sections BB and CC are due to the different dimensions, forms and material characteristics. In static condition, for both sections, the presence of the ship increases the displacements of about three times with respect to absence of the ship condition.

As example of the output, for the three sections AA, BB and CC, Fig. 22 shows the vertical stresses for the ending excavation and backfilling phases.

The presence of the drainage galleries in section BB is not relevant to the overall behavior because of their small dimensions. In fact, it results that the section CC (without the galleries) is afflicted by a more severe stresses condition in correspondence of the points A and B with respect to section BB (Figs. 20 and 21). Moreover, the stresses in the galleries' crowns are smaller than the corresponding conglomerate strength (Fig. 23).

4.4.3. Eigenfrequency analysis

Referring to the sections BB and CC (respectively representing the old dry dock and the new dry dock), the analysis is performed by highlighting the different vibration modes of the structure. The obtained values of natural vibration periods, in the case of empty basin, are given in Table 13.

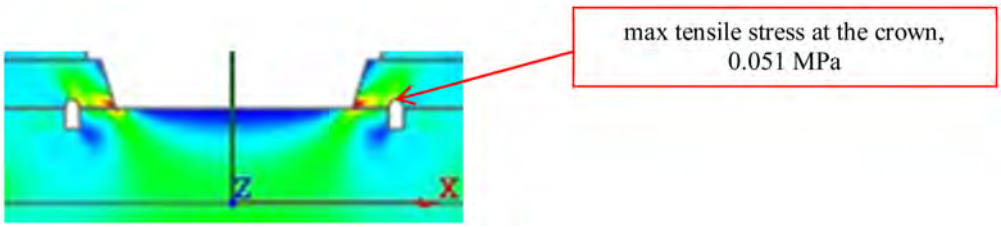

Fig. 23. Drainage galleries.

Table 13
Natural vibration periods.

Mode	old dry dock		new dry dock	
	without ship [s]	with ship [s]	without ship [s]	with ship [s]
1°	0.50	3.11	0.45	3.11
2°	0.38	0.50	0.37	0.37
3°	0.28	0.38	0.26	0.26
4°	0.27	0.28	0.25	0.25
5°	0.26	0.27	0.23	0.23
6°	0.23	0.26	0.21	0.21
7°	0.19	0.23	0.19	0.19

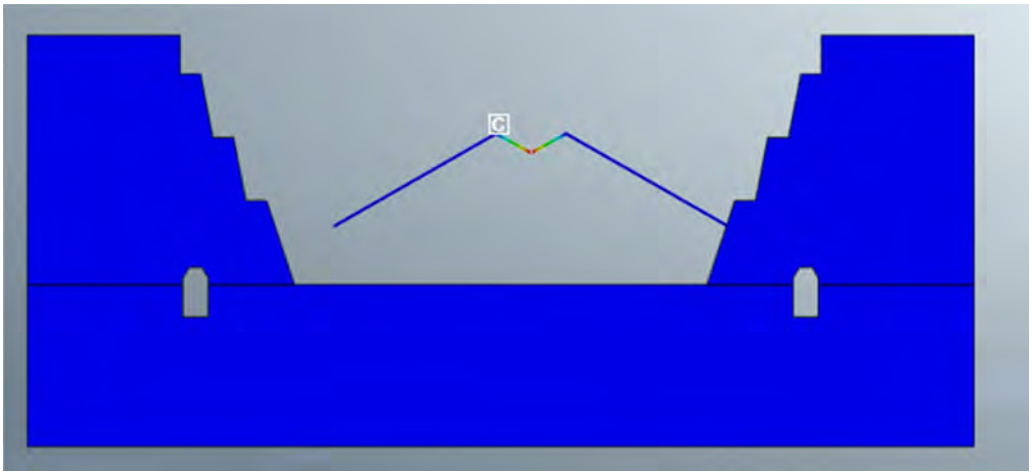

Fig. 24. Vibration mode shape involving only the ship.

In the case in which the ship is in-maintenance inside the basin, a further vibration mode appears having period of about 3.11 s (higher than the first period of the old dry dock, 0.50 s, and the first period of the new dry dock, 0.45 s). This mode involves only the ship mass as shown in Fig. 24 (thus the vibration mode of the ship is decoupled with respect to the vibration modes of the structure).

4.4.4. Dynamic analysis considering the soil-structure interaction

The analysis is performed by using the direct integration of the motion equation in the time domain, considering ground motion time histories of 20 s. The present analysis is repeated for all the three above described characteristic sections. The seismic action is defined as a combination of the three components along the principal axis of the structure, as required by Ref. [12]:

$$E = \left(\pm E_x \pm 0.3 \cdot E_y \pm 0.3 \cdot E_Z\right)$$

The Tables 14–16 show the maximum values of displacements and stresses detected in the time history results obtained by the FEM integration of the motion equations under the three orthogonal ground accelerations time histories.

The maximum stress-strain value found in correspondence of the point "A" (at intrados of the foundation plane, in the section AA) could be considered critical, that is indicative for the behavior of the dry dock section. As it is highlighted from the previous tables, the three sections are afflicted by increments of stresses and deformations due to the seismic action

Table 14
Seismic analysis in "soils+structure" case: displacements and stresses evaluated in the remarkable points of section AA

Points	Section AA					
	Dx [mm]	Dy [mm]	Dz [mm]	Δσxx [MPa]	Δσyy [MPa]	Δσzz [MPa]
A	−26.42	−1.56	−0.23	−0.061	−0.082	−0.024
B	−26.09	−1.56	−0.16	0.056	−0.120	−0.036
C	−28.37	−2.00	−0.23	0.561	0.009	−0.047
D	−28.25	−2.08	−0.23	−0.569	−0.104	0.0500
E	−27.57	−2.52	−0.28	−0.047	−0.144	0.003
F	−27.58	−2.43	−0.25	−0.042	0.148	0.003

Note: displacements: the negative values represent a downwards displacements; stresses: the negative values represent compression stresses.

Table 15
Seismic analysis in "soils+structure" case: displacements and stresses evaluated in the remarkable points of section BB.

Points	Section BB				
	Dx [mm]	Dy [mm]	Δσxx [MPa]	Δσyy [MPa]	Δσxy [MPa]
A	27	−15	0.018	0	0.020
B	26	−15	0.006	0	0.028
C	31	−15	0.035	0	0
D	31	−15	0.003	0.003	0
E	29	−15	0.056	0.064	0.053
F	29	−16	0.062	0.025	0.060

Note: displacements: the negative values represent a downwards displacements; stresses: the negative values represent compression stresses.

Table 16
Seismic analysis in "soils+structure" case: displacements and stresses evaluated in the remarkable points of section CC.

Points	Section CC				
	Dx [mm]	Dy [mm]	Δσxx [MPa]	Δσyy [MPa]	Δσxy [MPa]
A	26	−15	0.013	0	0.016
B	26	−15	−0.020	0	−0.031
C	29	−15	0.004	1	0
D	29	−15	−0.004	1	0
E	27	−15	0.023	0.018	0.038
F	28	−15	−0.022	−0.021	0.039

Note: displacements: the negative values represent a downwards displacements; stresses: the negative values represent compression stresses.

in comparison to the static condition results; the values obtained in the seismic analysis are widely compatible with the stresses and displacements occurred in the dry dock conventional loading-unloading conditions.

As example of the output, for the points A and B of the three sections AA, BB and CC, Fig. 25 shows the time history results in terms of σ_{yy} (vertical stresses).

The different dynamic behaviors obtained for the old dry dock (including the sections AA and BB) and the new dry dock (including the section CC) justify the cracks actually present in the joint between the old and the new parts (for the existing cracks, see also Fig. 26).

5. Conclusions

The results of the static analysis show that the structure of the dry-dock (built in conglomerate) is able to provide the necessary structural safety in service conditions. However, on the basis of the conglomerate characteristics, this safety could not be guaranteed for a long time due to the damaging phenomena affecting the durability of the materials (e.g. fatigue stresses caused by the loading-unloading-reloading cycles which daily afflict the dry dock during its serviceability conditions).

This consideration is valid for the structures of the basement (either in the old and new dry dock) and in particular for the *gargame area,* close to the mentioned ship-lock.

Therefore, as it is shown by the different analyses of the three cross sections AA, BB and CC, structural problems afflict the side walls of the basin due to the differential displacements between these sections.

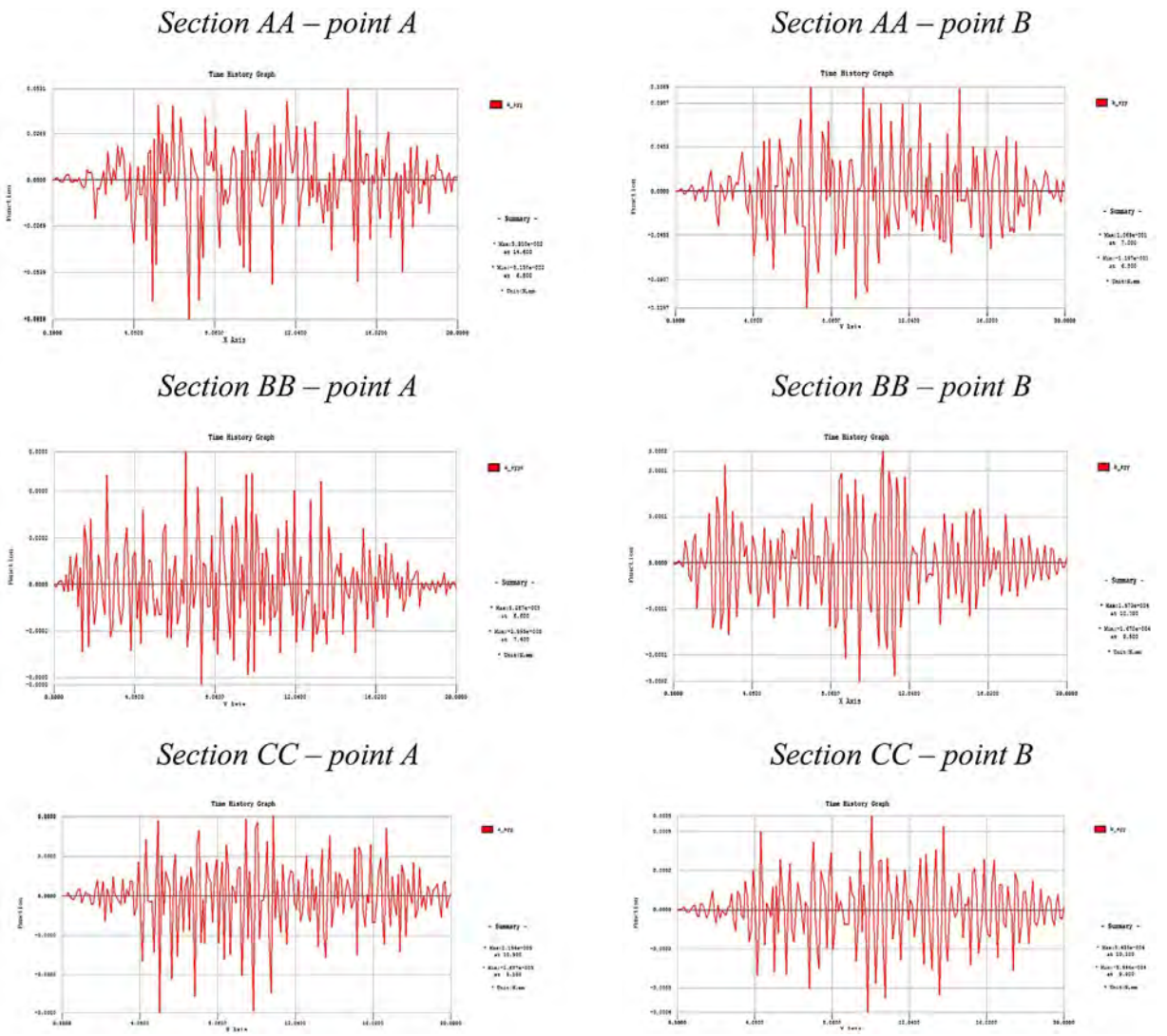

Fig. 25. σyy-time history results for the points A and B of the sections AA, BB and CC [MPa, s].

Moreover, the region of the "old dry dock" presents stresses which are largely compatible with the estimated strength of the materials. On the contrary, the structural situation of the "new dry dock", characterized by the presence of many cracks and the consequent water seeping, means that the on-site stress fields are not compatible with the mechanical characteristics of the materials. Furthermore, the differences in terms of stresses between section BB and CC are due to many causes: the different geometry, the different materials (concrete in CC and stone masonry in BB) and the different influence of the crane load (the crane is closer to CC side walls than the BB ones). Thus, the effect of the drainage galleries on the stress fields is less relevant with respect to the mentioned causes.

On the basis of the performed seismic analyses and as confirmed by what happened in the past earthquake (in 1908), the presence of the ship located in the dry dock basin represents an instability condition. This occurs because the ship (present in the sections BB and CC) is simply supported on the docking blocks. In case of earthquake, the structural vibrations of the structure and the ship are decoupled and, in extreme case, the overturning of the ship on the dock's walls could be possible because no other connections between the ship and the structure are present.

The compression and tensile stresses obtained in the static and dynamic analyses are compatible with respect to the strength of the dry dock materials. Nevertheless, owing to the expectable increase of damage due to durability problems, these stresses could be not acceptable in the future. Furthermore, the stress fields in the structure do not show excessive concentrations; this could be helpful in the planning of the rehabilitation works that will interest only limited and well-identified regions, in order to eliminate the flaw of the structural materials.

Fig. 26. Existing cracks in walls of Section CC (the most evident in red).

References

[1] B.K. Mazurkiewicz, Design and Costruction of Dry Drocks, Trans Tech Publications, Rockport (USA), 1980.
[2] Gregory P. Tsinker, Handbook of Port and Harbour Engineering: Geotechnical and Structural Aspects, Springer-Science+Business Media, B.V, 1997.
[3] P. Kavitha, M. MuthuVenkatesh, R. Sundaravadivelu, Soil Structure Interaction Analysis of a Dry Dock, International Conference on Water Resources, Coastal and Ocean Engineering (ICWRCOE 2015) (2015).
[4] A.O. Awojobi, R.E. Gibson, Plane strain and axially symmetric problem of a linearity non homogeneous half-space, Quart. J. Mech. Appl. Math. 26 (1973) 285–302.
[5] R. Nova, Meccanica delle costruzioni geotecniche. Città Studi Edizioni, (2008).
[6] S.L. Kramer, Geotechnical Earthquake Engineering, Prentice Hall, Upper Saddle River, New Jersey (USA), 1996.
[7] Y. Ohta, N. Goto, H. Kagami, K. Shiono, Shear wave velocity measurement during a standard penetration test, Earthquake Eng. Struct. Dyn. 6 (1) (1978) 43–50.
[8] R. Lancellotta, Geotecnica, Zanichelli, Bologna (Italy), 1994.
[9] A.K. Chopra, Dynamics of Structures., Prentice Hall, Upper Saddle River, New Jersey (USA), 1995.
[10] H. Poulos, E. Davis, Elastic Solutions for Soil and Rock Mechanics, Wiley, 1974.
[11] Analysis reference MIDAS GTS NX.
[12] Norme Tecniche per le Costruzioni, D.M. 14 gennaio 2008 —NTC 2008.
[13] SIMQKE_GR software, version 2.7—http://dicata.ing.unibs.it/gelfi/software/simqke/simqke_gr.htm.
[14] R. Lancellotta, D. Costanzo, S. Foti, Progettazione geotecnica, HOEPLI, Milan (Italy), 2011.
[15] Yan Shu-wang, Liu Ke-jin, Analysis of dry dock slope stability at different construction stages, in: Mechanic Automation and Control Engineering (MACE), 2010 International Conference, 2010.
[16] G. Riga, Modellazione geologica e geotecnica, Dario Flaccovio Editore, Palermo (Italy), 2011.